IUST
Iran University of Science and Technology

Iranian Journal of Electrical and Electronic Engineering

Journal Homepage: ijeee.iust.ac.ir

Wide-Band Dynamic Load Generator for Emulation of Complex Nonlinear Characteristics of Industrial Loads

H. Azizi Moghaddam(C.A.)* and A. Farhadi**

Abstract: Dynamometers are equipment that has been widely used in the field of electric machines test benches. A dynamometer system has the ability to create intricate and unpredictable behaviors of mechanical loads according to a programmed manner. Extensive research into the characteristics of loads found in industrial settings has shown that non-linear and complex phenomena, including misalignment, mechanical friction, and others, are unavoidable in industrial drive systems. To assess the performance of motor and drive systems in industrial drives when subjected to these non-linear and complex loads, a fast and precise dynamic drive system must track high-frequency torque signals with precision. The suggested dynamometer, serving as an instrumental device, has the ability to emulate a wide torque response across various frequencies during both transient and steady-state conditions for the machine under test. Simulations and experimental results confirm the dynamometer's wide-ranging dynamic response, enabling the emulation of different linear and non-linear loads.

Keywords: wide-band dynamometer, dynamic load emulation, nonlinear loads, misalignment, crankshaft.

1 Introduction

AN advanced electrical motor test bench is a software and hardware tool to analyze the performance characteristics of an electrical machine under different loads which exhibit nonlinear and complicated behaviors. The main part of a test bench is the dynamometer which consists of three building blocks: an electrical machine, a drive system, and measuring sensors. In fact, a dynamometer is aimed to emulate dynamic and static characteristics of the desired mechanical loads. Moreover, there are some sort of nonlinear phenomena such as backlash, misalignment, mechanical resonance, etc., that need to be taken into account in the motor test benches. Using a mechanical load emulator is mandatory for performing programmable tests with the lowest cost and the highest accuracy.

The mechanical load characteristics encompass various components, including static torque, dynamic torque, and non-linear aspects. Over the past few decades, several types of dynamometers have been introduced to the market, each with its own limitations. Dynamometers like eddy current, magnetic powder, hysteresis, and hydraulics are primarily used for testing motors in specific regions, namely the first and third regions. Additionally, these dynamometers are only suitable for emulating static torque components and are not designed for dynamic torque emulation.

A referenced dynamometer [1] possesses dynamic torque emulation capabilities, but it relies on a DC motor for emulation. However, DC motors have inferior speed dynamic response compared to AC motors, making them unsuitable for modern-generation dynamometers. The new generation of AC dynamometers offers significant advantages over traditional types. Apart from their ability to regenerate brake power back to the network, AC dynamometers exhibit a fast dynamic response that allows them to accurately emulate the dynamic

Iranian Journal of Electrical & Electronic Engineering, 2024.
Paper first received 31 May 2023 and accepted 28 February 2024.
* The author is with the Rotating Electrical Machines Research group, Niroo Research Institute, Tehran, Iran.
E-mail: hmoghaddam@nri.ac.ir.
** The author is with the Rotating Electrical Machines Research group, Niroo Research Institute, Tehran, Iran.
E-mail: afarhadi@nri.ac.ir & farhadi.arman71@gmail.com.
Corresponding Author: H. Azizi Moghaddam.

characteristics of complex and non-linear mechanical loads. In reference [2], the AC dynamometer emulates linear loads and does not consider non-linear loads. On the other hand, dynamometers mentioned in references [3]-[8] emulate only a specific type of non-linear load and neglect other linear and non-linear loads. References [9]-[11] demonstrate the AC dynamometer's capability to emulate various non-linear loads. However, some of these loads are not commonly encountered in industrial drives and are merely hypothetical non-linear loads.

The load torque in electrical drive systems is conventionally classified into six groups: constant, frictional, quadratic, constant power, path-dependent, and rotor angle-dependent, as stated in reference [12]. Additionally, different non-linear loads in electrical drive systems are classified in reference [13]. Since a dynamometer serves as instrumental equipment, the driver system it employs must offer both high precision and a rapid dynamic response for torque in both transient and steady states. After evaluating the performance of the dynamometer's drive system in torque and speed control modes, the torque control method is chosen due to its fast dynamic response and wide-ranging capability. This paper presents the simulation and experimental results of a proposed AC dynamometer that possesses the ability to emulate various types of non-linear loads with different bandwidths. The results obtained demonstrate the dynamometer system's capability to load both static and dynamic characteristics effectively. Notably, the implemented dynamometer system has the advantage of being able to load complex mechanical loads, such as misalignment and crankshaft loads. In addition to the hardware implementation, a software environment is provided, enabling the configuration of various test scenarios, device protection, data acquisition, data processing, and data extraction. Consequently, the specifications of the proposed dynamometer can be summarized as follows.

- The ability to test motors in all four regions of the speed-torque characteristic.
- The capability to emulate both static and dynamic components of the load torque.
- High flexibility in implementing different scenarios and combining various load characteristics.
- The ability to emulate non-linear components and handle complex industrial loads.

2 The Control Approach of Proposed Dynamometer

The dynamometer consists of three building parts including an electrical machine as a dynamometer, power electronic converters, and measuring sensors. Fig. 1 shows the control approach of the dynamometer, which is based vector method. In this method, the motor speed ω_r is measured, and the instantaneous value of the torque, based on the analytical relation between the torque and speed, is calculated and applied to the dynamometer's driver system as the reference torque T_e*. The dynamometer drive system must track the desired reference torque. The reference torque value, from an exterior loop, is calculated based on Eq. (1) and applied to the FOC controller, as shown in Fig. 2. The inverter voltage reference V^*_{abc} is obtained after reference currents calculation along the two axes dq using the current controllers. Finally, the modulator provides the inverter switching PWM pulses based on the calculated reference voltages. In this approach, the measured motor speed ω_r is applied to the coupling model to obtain the speed $\omega_{r'}$. The coupling model can emulate the coupling system's non-linear effects. In the case of neglecting the coupling model, then ω_r will be equal ω_r.

Considering the effects of linear and non-linear loads, the reference torque T_e* of the FOC method is calculated as:

$$T_e^* = f(\omega_r) = T_{demand} \tag{1}$$

$$T_{demand} = \pm T_0 \pm a_1\omega_r \pm a_2\omega_r^2 \pm a_3\omega_r^3 \pm \ldots \pm J_{demand}\frac{d\omega_r}{dt} + T_{nl}$$

where, T_{demand} is the requested load torque, T_{nl} is the non-linear torque of the load, T_0 is the constant torque component of the load, a_1, a_2, ... is the coefficient of the load torque function, and J_{demand} is the requested inertia of the load. Therefore, by defining parameters: T_0, a_1, a_2, …, J_{demand} and T_{nl}, the reference torque value T_e* is calculated in terms of the speed of the axis between the motor and dynamometer and is applied to the vector control method.

3 Simulation results

This section discusses the simulation of several non-linear loads by the AC dynamometer. The torque control method, as shown in Fig. 1 and Fig. 2, is used for controlling the dynamometer. The dynamometer's motor is an induction motor with the parameters defined in Table 1. Also, an induction motor with the parameters of Table 1 is connected to the dynamometer as the motor under test. Fig. 3 shows the simulation results of the dynamometer's step response for the nominal torque value of 13 N.m. As can be seen, the dynamometer tracked the reference step well as a result of the system's fast dynamic response. Furthermore, the ability of fast dynamic response allows the dynamometer to emulate the non-linear load torques with the different scenarios.

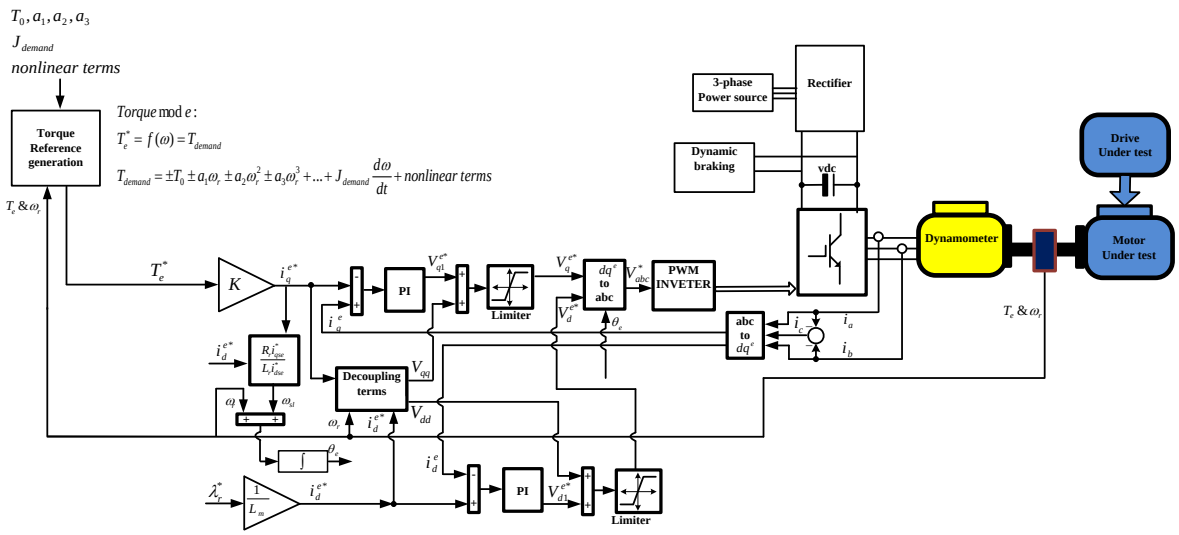

Fig. 1 Block diagram of dynamometer control according to FOC method

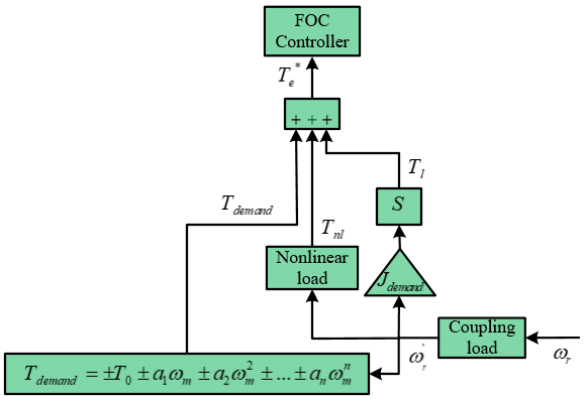

Fig. 2 Block diagram of dynamometer control according to FOC method.

Table 1 The dynamometer and motor under test parameters

Parameters	Dynamometer motor	Motor under test
Nominal power	4 kw	4 kw
Nominal voltage	380 V	380 V
Nominal speed	2880 rpm	2890 rpm
Pole pairs	1	1
Nominal current	7.6 A	8.17 A
The moment of inertia	0.046 kg/m2	0.046 kg/m2
Dynamometer PI regulator coefficient	Kp-torque=10000,Ki-torque=10,Kp flux=1000andKi- flux =1	

In the first scenario, the dynamometer must emulate a sinusoidal load torque with 5 N.m amplitude and a frequency of 40 Hz for the motor under test. The simulation results of this scenario are shown in Fig. 4. As can be seen, the dynamometer is capable of tracking the sinusoidal reference torque with a fast dynamic response. Therefore, the dynamometer can emulate any load torque with high-frequency non-linear components.

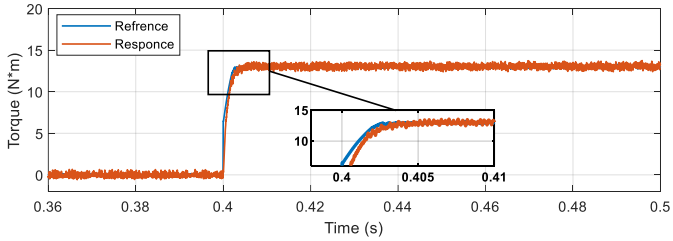

Fig. 3 The step response of the dynamometer

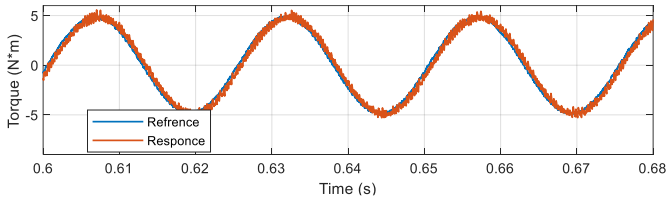

Fig. 4 The dynamic response for 40 Hz sinusoidal torque

In the second scenario, the dynamometer must simulate the misalignment load torque. Fig. 5 shows the misalignment load model. In the misalignment load model, the motor under the test shaft is connected to the load with the angle β, which causes unwanted sinusoidal torques in the system. The reference [14] provides a more detailed analysis of misalignment load torque relationships. Since misalignment load torque is of the coupling type, it converts the measured speed of the motor ω_r to the coupling speed $\omega_{r'}$ by the following relation:

$$\omega_r' = \frac{\cos(\beta)}{1-\sin^2(\beta)\cos^2(\theta_r)}\omega_r \quad (2)$$

where the angular position of the load motor can be denoted as $\theta_r = \omega_r t$.

Fig. 6 shows the result of the misalignment load torque simulation for the dynamometer. Here, the angle β=5° is considered. The simulation scenario is that at the moment 0.6 s, the system speed has increased from 2500 rpm to 2900 rpm. The dynamometer emulates misalignment load torque accurately at 2500 rpm and 2900 rpm steady state speeds.

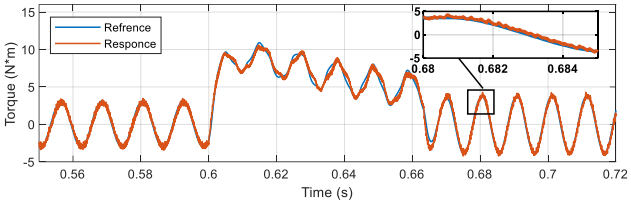

Fig. 6 Misalignment load simulation results

In the third scenario, the crankshaft load torque, which has a more complex non-linear behavior, is investigated. Fig. 7 shows the model of the crankshaft mechanical load. Compressors, equipped with drive systems, are one of the loads that indicate the crankshaft mechanism.

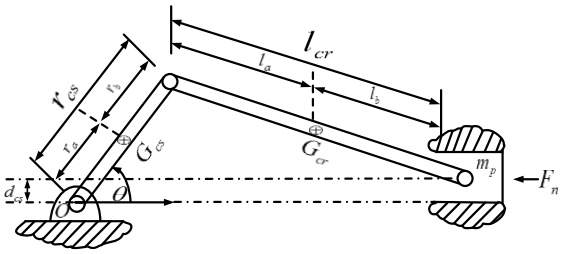

Fig. 7 The model of crankshaft load

In the crankshaft mechanism, the relation between the load's torque with the speed, position, inertia, and other geometrical parameters are modeled as follows:

$$T_{nl} = (J_m + J_{cs}(\theta_r))\frac{d\omega_r}{dt} + F_n r_{cs}\left(\sin(\theta_r) + \frac{\frac{r_{cs}}{l_{cr}}\sin(2\theta_r)}{\sqrt{1-(\frac{r_{cs}}{l_{cr}}\sin(\theta_r))^2}}\right) \quad (3)$$

where J_m, F_n, l_{cr}, and r_{cs} are the motor moment of inertia, the normal force, the connecting rod length, and the crank length, respectively. The term $J_{cs}(\theta_r)$ $\theta_m = \omega_m . J_{cs}(\theta_m)$is the inertia moment of the crankshaft mechanism, which is not considered here for simplicity [15].

Fig. 8 shows the simulation result of the crankshaft load. The simulation scenario is such that at the beginning, the reference speed of the motor is 1000 rpm, and at the instant of 0.6 s, the speed has increased to 2300 rpm. At 1000 rpm and 2300 rpm, the dynamometer tracked the torque reference very well.

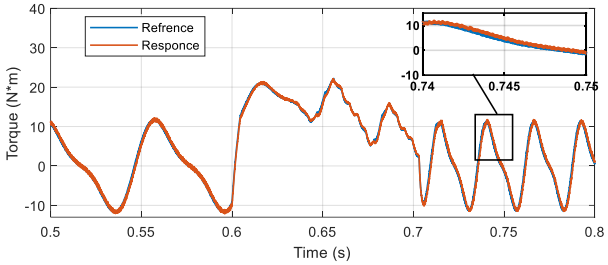

Fig. 8 Crankshaft load simulation results

4 Experimental results for linear loads

In this section, some linear loads are emulated by the proposed dynamometer. Fig. 9 shows the experimental implementation of the dynamometer system. The controlling algorithm is programmed on a DSP TMS320f335 processor. The motor under test is controlled using EUROTHERM drive AC690. The drive of the motor under test is based on the V/F method. The dynamometer motor and the motor under test parameters are indicated in Table 1. The sampling rate of electrical signals is 10 kHz and the update rate of FOC control method calculations in the DSP processor is 110 microseconds. The switching frequency of inverter is about 10 KHz.

In the experimental setup, the RT2A sensor used to measure dynamic torque. Also, the voltage and current of test system measured by the LV25P and LA55P hall effect sensors.

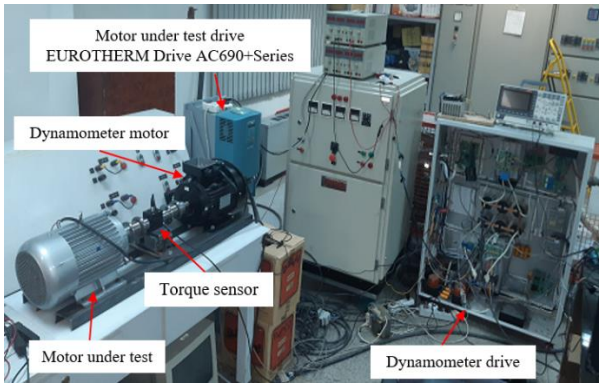

Fig. 9 The experiment platform of proposed dynamometer

4.1 Constant load torque emulation

The system response to the pulse torque reference in the second and third regions of the torque-speed characteristic is investigated in this section. Fig. 10 shows the pulse torque reference T0=±3 N.m (yellow curve), the dynamometer motor torque (blue curve), and the stator current. As can be seen, the dynamometer motor torque tracks the instantaneous reference torque accurately. Based on experimental results, the speed of the dynamic response is approximately equal to 30 msec.

Non-linear behaviors of mechanical loads can lead to the high frequency torque fluctuations. The ability to generate high frequency components of the load torque is largely influenced by the dynamic response speed of the dynamometer. The quick response speed of the dynamometer depends on the current and torque limits of the motor in addition to the system dynamics. The initial values of PI coefficients were determined by using the well-known Ziegler-Nichols method. Then the final values of PI coefficients tuned base on the Trade–off between dynamic response, over shot and stealing time.

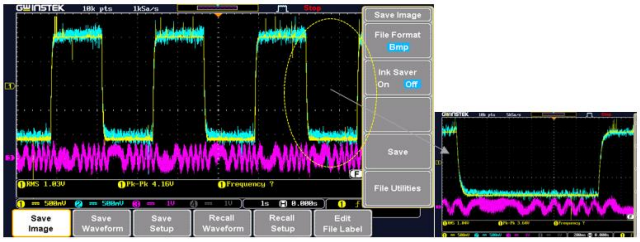

Fig. 10 The dynamometer torque response for the pulse torque reference T_0=±3 N.m

4.2 Constant load torque emulation

Programmable loading of the motor under test based on the user-selected torque profile can be considered one of the advantages of the dynamometer system. Fig. 11 shows the motor under test speed (yellow curve), load brake torque (blue curve), and motor stator current (motor under test current) in the condition of applying a step-wise load brake torque from the no-load state to the nominal load state. Therefore, this ability allows an automatic motor testing operation as if when reaching the steady-state condition, the electrical and mechanical quantities are measured, the required data are extracted, and this procedure is repeated for each step of the load torque changes. Finally, by connecting the obtained points, the required characteristic is extracted. In this method, the number of steps and the interval time between applying the torque moments are programmable. Moreover, if the number of steps is increased (for small step sizes), the load torque profile will be a ramp function, where the rate of the slope and the peak of the torque is programmable. The braking energy have been dissipated in a dynamic braking (resistor parallel to the dc bus) such that the DC voltage limited in safe range.

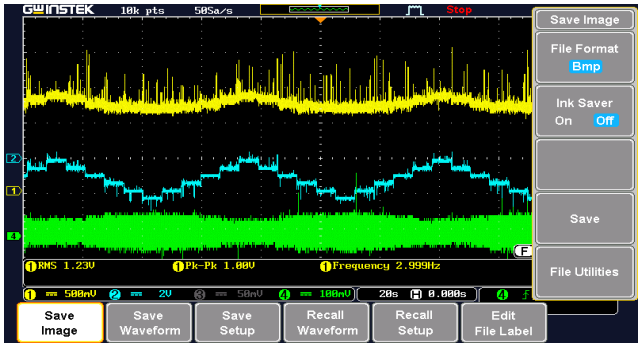

Fig. 11 In order from the top: motor under test speed, dynamometer torque, and motor under test current for the programmable load T_0=±12 N.m

4.3 Frictional torque and programmable frictional and fan type

In this scenario, the dynamometer is used to test friction and fan loads as two common types of industrial loads. The following equations represent the torque and speed characteristics of the two tested loads in this scenario.

$$T_{fric} = k_{fric}\omega_r \tag{4}$$

$$T_{fan} = k_{fan}\omega_r^2 \tag{5}$$

Fig. 12 displays the motor speed under test (yellow curve), the dynamic break resistance current (red curve), the dynamometer brake torque (blue curve), and the stator current of the motor under test (green curve) for the friction torque profile at k_{fric}=0.02. In this test, the speed of the motor under test is varied by the user through the control panel settings of the drive. With the change in speed, the reference torque value applied to the dynamometer drive system is calculated based on Eq. (4). The calculated torque signal is sent as a reference torque to the dynamometer control. As shown in Fig. 12, the brake torque generated by the dynamometer motor (blue curve) is applied to the motor under test. As can be seen, the applied load torque profile is in line with the speed of the motor under test, so that with the increase in speed, the friction load torque also increases. In this case, changes in the stator current waveform of the motor under test are fully aligned with the torque loading of the motor under test. As can be seen in Fig. 12, with a decrease in the inertia of the load, the torque dynamics of the dynamometer and the speed of the tested motor are affected by the low inertia of the load. In this case, the effect of ripple torque damping through load inertia is reduced, which leads to an increase in mechanical vibrations and increased acoustic noise.

In the laboratory modeling process, a widely encountered load in the industry, known as a fan load, is being examined. To conduct this investigation, Eq. (5) is

utilized as a reference, providing the necessary framework or equation to follow. The fan load torque is produced with k_{fan}=0.000033 and applied to the dynamometer drive system. In this test, the test motor speed is varied by the user using the drive system. In this case, for each speed, a reference torque value is calculated based on Eq. (5) and sent to the dynamometer drive system. Fig. 13 shows the test motor speed (yellow curve), dynamic brake current, dynamometer brake torque, and phase A motor current under load conditions of the fan load. As expected, the produced brake torque by the dynamometer system is proportional to the square of the speed, and the effect of this loading is clearly visible on the stator current waveform of the test motor.

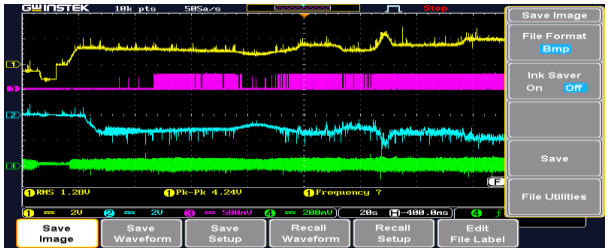

Fig. 12 In order from the top: motor under test speed, the injected current to the break resistor, the dynamometer torque, and the current of the motor for the frictional load

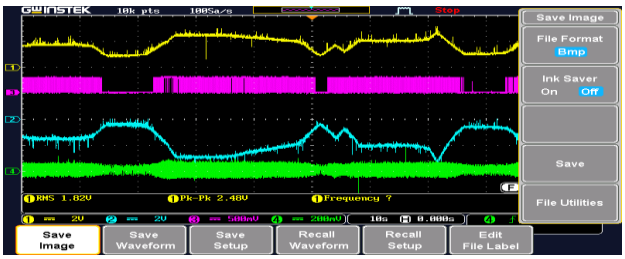

Fig. 13 In order from the top: motor under test speed, the injected current to the break resistor, the dynamometer torque, and the current of the motor for the fan load

4.4 Dynamic load torque emulation

The industrial load's torque is composed of two components of static torque T_{static} and dynamic torque, which is represented as follows:

$$T_l = T_{static} + J_{load}\frac{d\omega_r}{dt} \quad (6)$$

Here J_{load} and T_l are load inertia momentum and the load reference torque, respectively. Programmable loading of the dynamic torque effects resulting from the load inertia is one of the advantages of the proposed dynamometer. This capability of the dynamometer systems is utilized in many laboratory studies of motors and drivers, especially in electrical transportation applications. In this section, the load inertia effects on the dynamometer system-generated torque are tested experimentally. The dynamometer's motor, shown in Fig. 14, has inertia J_{dynamo}=0.046 kg/m2, which is added to the motor under test inertia. The system's dynamic equation when the motor under test is connected to the dynamometer motor is described as follows

$$T_M - T_{dynamo} = (J_M + J_{demand} + J_{dynamo})\frac{d\omega_r}{dt} \quad (7)$$

where J_M, J_{dynamo}, and J_{demand} are the motor under test inertia, the dynamometer's motor inertia, and the required reference inertia for loading on the motor, respectively. The T_M and T_{dynamo} express the motor under test inertia and the dynamometer's motor torque. The J_{demand} inertia value can be more or less than the J_{dynamo} value.

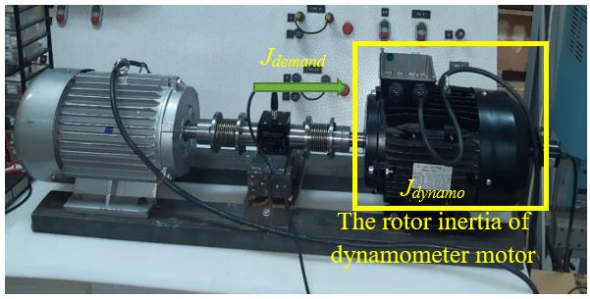

Fig. 14 Dynamometer motor and motor under test

Based on Eq. (4), and considering that the inertia of the dynamometer's motor rotor is imposed on the motor under test, the reference dynamic torque T_l, which has to be generated by the dynamometer's motor, is calculated as:

$$T_l = (J_{demand} - J_{dynamo})\frac{d\omega_r}{dt} \quad (8)$$

The experimental results for J_{demand} =4J_{dynamo} are shown in Fig. 15. In this condition, the dynamic torque value 3J_{dynamo}.$d\omega_r/dt$ is added to the static torque. This dynamic torque term appears in the dynamometer's motor-generated torque from moment A. Decreasing or increasing this torque component is equivalent to decreasing or increasing the load inertia for the motor under test. After the increase of the dynamic torque term by the dynamometer system, the motor's speed dynamic response is made faster under the influence of this dynamic torque term.

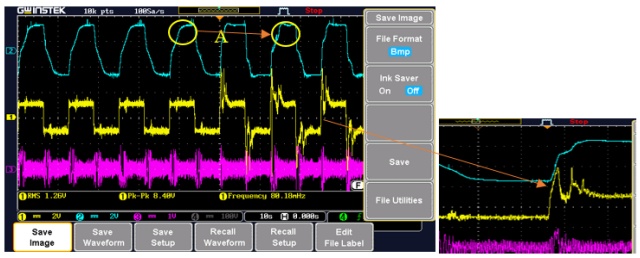

Fig. 15 In order from the top: motor under test speed, dynamometer torque, and motor under test current for the inertia J_{demand} =4J_{dynamo} and the pulse torque reference T_0=±3 N.m

5 Experimental results for nonlinear loads

In this section, the ability of the proposed dynamometer to emulate two linear loads has been investigated.

5.1 The determination of dynamometer bandwidth and the ability to generate high-frequency load torque components

The non-linear behavior of the industrial loads and the creation of unwanted high-frequency oscillations in the applied load torque into the motor drive system is unavoidable. These load torque components have typically high-frequency components, and the generation of these mechanical loads high-frequency components in the dynamometer's system needs the utilization of a drive system with a high dynamic response (high bandwidth). To evaluate the performance of the implemented control system for tracking the load torque high-frequency components, the dynamometer's drive system response for the sinusoidal reference torque ±3 N.m and the frequencies 1Hz to 40HZ is tested. The obtained results from the 1Hz and 40Hz tests are shown in Fig. 16 and Fig. 17, respectively, where the yellow color represents the reference torque signal, and the blue color expresses the dynamometer's torque. The experimental results show that the implemented drive system is capable of tracking the sinusoidal reference torque up to 40Hz with a fast and high precision dynamic. For the frequencies above 40Hz, the tracking error is increased dramatically, and the increase in the torque ripples causes the improper operation of the dynamometer system. To achieve higher bandwidths, using more complex controlling methods and higher switching frequencies is needed.

In order to ensure the correct operation of the dynamometer system, it is necessary that the ripple frequency components of the generated torque are far from the high frequency components of the dynamometer torque (caused by the non-linear behavior of the load). If the torque ripple components and dynamometer emulated torque fluctuation are close to each other, we will have a large error in the output torque of the dynamometer, which leads to an increase in the tracking error.

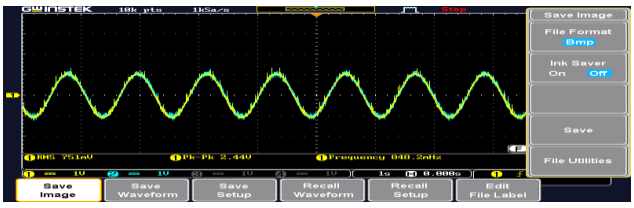

Fig. 16 The dynamic response of the dynamometer for 1 Hz sinusoidal reference torque

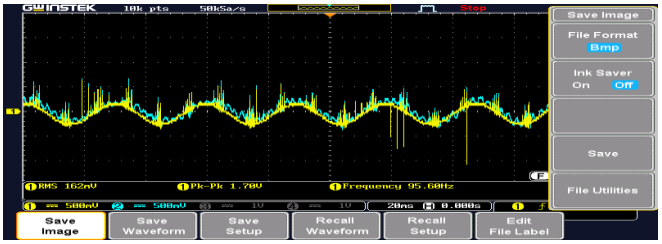

Fig. 17 The dynamic response of the dynamometer for 40 Hz sinusoidal reference torque

5.2 Misalignment torque emulation

One of the special capabilities of the proposed dynamometer is that the user can change the oscillatory torque parameters resulting from the misalignment load to observe its effects on the operation of the motor drive system. In the simulation results section, the mathematical relations and misalignment load torque waveforms are investigated. The experimental results for the misalignment load with $\beta=60^{\circ}$ is shown in Fig. 18. In this paper the angular misalignment has been simulated and implement. In this scenario, the misalignment load is applied at the moment T1. The experimental results show that, by the increase in the misalignment angle, the load's torque oscillation are increased, where the effects of these high-frequency fluctuations on the motor under test speed can be observed as the oscillations with the same frequency.

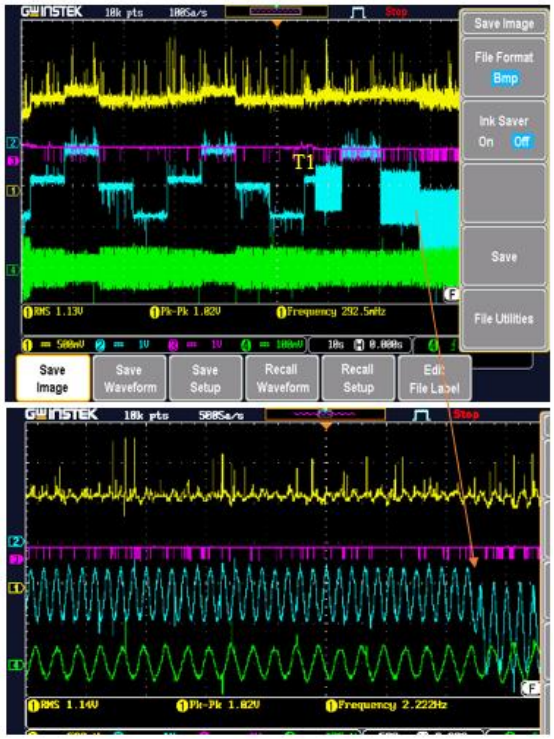

Fig. 18 In order from the top: motor under test speed, dynamometer torque, and motor under test current for the misalignment with $\beta=60^{\circ}$

5.3 Crankshaft mechanism torque emulation

As discussed in the simulation results, the crankshaft load has a complex behavior, and the dynamometer can emulate that on the motor under test. Fig. 19 shows the experimental results for the crankshaft load. In this scenario, the oscillatory component resulting from applying the crankshaft load is applied to the motor under test from the moment T_1. As represented in the experimental results (the enlarged section of Fig. 19), the dynamometer's torque control system, in addition to the load static torque, generates the oscillatory torque value resulting from the crankshaft load from the moment T_1. The effects of oscillatory components of the crankshaft torque on the motor under test speed and the stator current are considerable. Furthermore, Fig. 19 shows the dynamometer system behavior in the condition of the changes of the motor under test speed. The crankshaft load torque is dependent on the position and the derivatives of the speed, where the oscillation frequency and its amplitude are affected by the changes in the motor speed, as seen in Eq. (3). The effects of these oscillations on the transient speed response and the motor under test steady-state operation are shown in an enlarged view in Fig. 19.

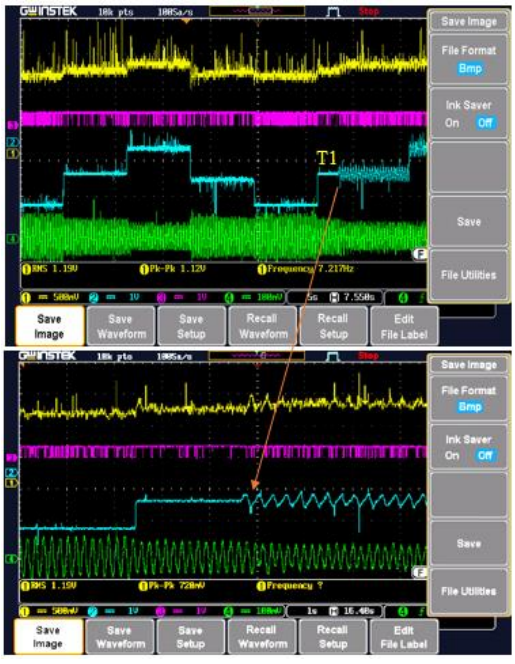

Fig. 19 In order from the top: motor under test speed, dynamometer torque, and motor under test current for the crankshaft load

6 Conclusions

This paper focuses on the implementation of various types of static loads, dynamic loads, and high-frequency non-linear components typically found in industrial loads. The dynamometer system and the response of the motor under test are evaluated and analyzed separately for each case. The analysis of the results demonstrates that the implemented dynamometer is capable of effectively modeling a wide range of industrial load characteristics in a laboratory setting. Both simulation and experimental results indicate that the proposed dynamometer exhibits a fast dynamic response. This feature proves particularly useful for emulating non-linear components in the frequency range of 1Hz to 40Hz, which are commonly present in loads such as misalignment or crankshaft loads. With the proposed dynamometer system, users can programmable load various combinations of static, dynamic, and non-linear components onto the motor under test, allowing for a detailed analysis of the motor drive system being examined.

References

[1] Hewson C. R., Sumner M., Asher G. M., and Wheeler P. W., "Dynamic mechanical load emulation test facility to evaluate the performance of AC inverters". *Power Engineering Journal*, vol. 14, no. 1, pp. 21-28, Feb. 2000.

[2] Kyslan K. and Durovsky F., "Dynamic Emulation of Mechanical Load – An Approach Based on Industrial Drives Features". *Automatika*, vol. 54, no. 3, pp. 356–363, Sept. 2013.

[3] Rodic M., Jezernik K., and Trlep M., "Dynamic emulation of mechanical loads: an advanced approach". *IEE Proceedings - Electric Power Applications*, vol. 153, no. 2, pp. 159-166, Sept. 2006.

[4] Arellano-Padilla J., Asher G. M., and Sumner M., "Control of an AC Dynamometer for Dynamic Emulation of Mechanical Loads with Stiff and Flexible Shafts". *IEEE Transactions on Industrial Electronics*, vol. 53, no. 4, pp. 1250-1260, June 2006.

[5] Bagh S. K., Samuel P., Sharma R., and Banerjee S., "Emulation of Static and Dynamic Characteristics of a Wind Turbine using Matlab/Simulink," *2nd Inter. Conf. Power, Control and Embedded Systems*, pp. 159–166, Allahabad, India, 2012.

[6] Gan C., Todd R., and Apsley J. M., "Drive System Dynamics Compensator for a Mechanical System Emulator". *IEEE Trans. on Industrial Electronics*, vol. 62, no. 1, pp. 70–78, June 2015.

[7] Fajri P., Lee S., Prabhala V. A. K., and Ferdowsi M., "Modeling and Integration of Electric Vehicle Regenerative and Friction Braking for Motor/Dynamometer Test Bench Emulation". *IEEE Transactions on Vehicular Technology*, vol. 65, no. 6, pp. 4264-4273, June 2016.

[8] Song-Manguelle J., Ekemb G., Mon-Nzongo D. L., Jin T., and Doumbia M. L., "A Theoretical

Analysis of Pulsating Torque Components in AC Machines with Variable Frequency Drives and Dynamic Mechanical Loads". *IEEE Transactions on Industrial Electronics*, vol. 65, no. 12, pp. 9311-9324, June 2018.

[9] Akpolat Z. H., Asher G. M., and Clare J. C., "Experimental dynamometer emulation of nonlinear mechanical loads". *IEEE Transactions on Industry Applications*, vol. 35, no. 6, pp. 1367-1373, Dec. 1999.

[10] Hakan Akpolat Z., Asher G. M., and Clare J. C., "Dynamic emulation of mechanical loads using a vector-controlled induction motor-generator set" *IEEE Transactions on Industrial Electronics*, vol. 46, no. 2, pp. 370-379, April 1999.

[11] de Oliveira C. M. R., de Aguiar M. L., de Castro A. G., Guazzelli P. R. U., Pereira W. C. d. A., and Monteiro J. R. B. d. A., "High-Accuracy Dynamic Load Emulation Method for Electrical Drives" *IEEE Transactions on Industrial Electronics*, vol. 67, no. 9, pp. 7239-7249, Sept. 2020.

[12] S.K. Pillai, A First Course on Electrical Drives, 1nd ed. New Delhi: New Age International, 1990.

[13] AziziMoghaddam H., Farhadi A., and Mohamadian S., "Non-linearity Effects of Industrial Loads on Induction Motor Servo Drive System". *Iranian Journal of Electrical and Electronic Engineering*, vol. 18, no. 2, pp. 2046-2046, Nov. 2021.

[14] Bossio J. M., Bossio G. R., and De Angelo C. H., "Angular misalignment in induction motors with flexible coupling," *35th Annual Conference of IEEE Industrial Electronics*, pp. 1033-1038, Porto, Portugal, 2009.

[15] Chen B., Wu Y., and Hsieh F., "Estimation of Engine Rotational Dynamics Using Kalman Filter Based on a Kinematic Model". *IEEE Transactions on Vehicular Technology*, vol. 59, no. 8, pp. 3728-3735, Oct. 2010.

Hossein Azizi Moghaddam received the B.Sc. degree in electrical engineering from Shiraz University, Shiraz, Iran, in2001, and the M.Sc. and PhD. degrees in electrical engineering from Iran University of Science and Technology (IUST), Tehran, Iran, in 2004 and 2013, respectively. Currently, he is an assistant professor at rotating electrical machines group at Niroo Research Institute (NRI). His research interests include design and optimization of electrical machines, electrical machines drives and testing, and power electronics.

A. Farhadi was born in Khorramabad, Iran. received the M.Sc. degree in electrical engineering from K. N. Toosi University of Technology, Tehran, Iran in 2017. S. He is currently a Lecturer at Lorestan University, Khorramabad. His research interests include control of variable speed drives, dynamic load emulation, model predictive control, embedded programming, multilevel converters, and AC-to-AC converters.